evaporated to dryness. The residue was dissolved in water and subjected to enzymatic digestion with sv PDE (0.3 unit/mL) and calf intestine AP (100 units/mL) and then subjected to acid treatment (0.1 N HCl, 90 °C, 5 min). The HPLC peak at 15.4 min was collected and the fraction was concentrated to afford ca. 20 μg of pure material. HPLC conditions: Cosmosil $5C_{18}$ ODS column; 0.05 M ammonium formate containing 0-10% acetonitrile; linear gradient, 20 min; flow rate of 1.5 mL/min. The ^1H NMR spectrum and HPLC behavior of the product **3** were identical with those of the authentic sample: HPLC retention time, 19.2 min; ^1H NMR (D_2O, TSP) δ 2.42-2.55 (m, 2 H, $H_{2'}$), 4.40 (br s, 1 H, $H_{5'}$), 5.06-5.12 (m, 1 H, $H_{3'}$), 5.75-5.82 (m, 1 H, $H_{1'}$), 6.05 (br s, 1 H, $H_{6'}$), 8.04 (s, 1 H, H_2), 8.21 (s, 1 H, H_8); SIMS (positive ion) m/z 248 $(M + 1)^+$.

Stability of 5 under Acidic and Basic Conditions. A 20-μL sample of **5** (0.1 mM) was treated with 6 N HCl (90 °C, 1 h), and the solution was neutralized with 6 N NaOH and subjected to HPLC analysis. Neither formation of **4** nor the decomposition of **5** was observed. Another 20 μL of **5** (0.1 mM) was treated with 0.1 NaOH (90 °C, 5 min), and the solution was neutralized with 1 N HCl and then subjected to HPLC analysis. Neither formation of **4** nor the degradation of **5** was observed.

Acknowledgment. This work was supported by Grant-in-Aid for Priority Research from the Ministry of Education, Japan. We thank Dr. S. Shuto (Toyo Jozo Co., Ltd.) for providing 2'-deoxyneplanocin A. We also thank Dr. N. Sugimoto, Konan University, for measuring the thermodynamic properties of the oligonucleotide. We are also grateful to Nippon Kayaku and Yamasa Shoyu Corp. for providing PEM and nucleosides, respectively.

Theoretical Approach to Drug Design. 2. Relative Thermodynamics of Inhibitor Binding by Chicken Dihydrofolate Reductase to Ethyl Derivatives of Trimethoprim Substituted at 3'-, 4'-, and 5'-Positions

Joseph J. McDonald and Charles L. Brooks III*

Contribution from the Department of Chemistry, Carnegie Mellon University, Pittsburgh, Pennsylvania 15213. *Received August 9, 1990*

Abstract: The relative binding thermodynamics of trimethoprim [2,4-diamino-5-(3',4',5'-trimethoxybenzyl)pyrimidine] congeners to chicken dihydrofolate reductase are determined by free energy simulation methods. The congeners considered in this study represent methoxy to ethyl substitutions at the 3'-, 4'-, and 5'-positions of trimethoprim found at the benzyl portion of the inhibitor. Molecular dynamics simulations of the protein-inhibitor complexes, and the evaluation of potential energy interactions between inhibitor and protein, were evaluated for their ability to predict trends similar to those found for the thermodynamic simulations. The relative free energy trends for the 3',5'-diethyl and 3',4',5'-triethyl derivatives of trimethoprim follow those observed experimentally for identical inhibitor compounds. An observation of a reversal of enzyme preference for species with 3'- or 5'-ethyl functional groups, depending on the absence or presence of a 4'-ethyl group, demonstrates complex influences by active site atoms on the relative thermodynamics of inhibitor binding. Potential energy data derived from molecular dynamics of inhibitor-protein complexes show no demonstrable correlation to experimental results or calculated thermodynamic data.

Introduction

The process of inhibitor binding by proteins or enzymes is a complex thermodynamic one, which is driven by both energetic and entropic changes. Changes to the free energy of inhibitor binding, resulting from the addition or deletion of functional groups, arise from differences in the solvation/desolvation thermodynamics of the inhibitor and protein, energetic differences associated with different inhibitor-protein contacts, and conformational entropy changes to the protein and inhibitor.[1] Information regarding relative free energy differences between different inhibitors bound to a common receptor is accessible via experimental methods[2,3] or more recently with theoretical methods using the thermodynamic cycle perturbation (TCP) approach.[4-7] In addition, quantitative structure-activity relationship (QSAR) studies can be used to augment thermodynamic data.[16] In this article, free energy simulation methods are used to investigate the principles that determine the structural and thermodynamic aspects of inhibitor binding and specificity. In particle, with this work we extend earlier thermodynamic simulations for the binding of trimethoprim [2,4-diamino-5-(3',4',5'-trimethoxybenzyl)pyrimidine] and congeners to dihydrofolate reductase (DHFR) derived from chicken liver.[5,8,9] This system is a strong candidate for testing the utility of these methodologies given the number of crystallographic structures for DHFR derived from several species,[10-14] and the experimental characterization and QSAR analyses of inhibitor-DHFR complexes,[15,16] as well as the importance of DHFR as a target for inhibition in the treatment of bacterial

(1) Beveridge, D. L.; DiCapua, F. M. *Annu. Rev. Biophys. Biophys. Chem.* **1989**, *18*, 431.
(2) Mares-Guia, M.; Nelson, D. L.; Rogana, E. *J. Am. Chem. Soc.* **1977**, *99*, 2336.
(3) Craik, C. S.; Langman, C.; Fletcher, T.; Rocznick, S.; Barr, P. J.; Fletterick, R.; Rutter, W. J. *Science* **1985**, *228*, 291.
(4) Fleischman, S. H.; Brooks, C. L. *J. Chem. Phys.* **1987**, *87*, 3029.
(5) Fleischman, S. H.; Brooks, C. L. *Proteins* **1990**, *7*, 52.
(6) Wong, C. F.; McCammon, J. A. *J. Am. Chem. Soc.* **1986**, *108*, 3830.
(7) Bash, P. A.; Singh, U. C.; Brown, F. K.; Langridge, R.; Kollman, P. A. *Science* **1987**, *235*, 574.
(8) Brooks, C. L. *Int. J. Quantum Chem., Quantum Biol. Symp.* **1988**, *No. 15*, 221.
(9) Brooks, C. L.; Fleischmann, S. H. *J. Am. Chem. Soc.* **1990**, *112*, 3307.
(10) Bolin, J. T.; Filman, D. J.; Matthews, D. A.; Hamlin, R. C.; Kraut, J. *J. Biol. Chem.* **1982**, *257*, 13650.
(11) Matthews, D. A.; Bolin, J. T.; Burridge, J. M.; Filman, D. J.; Volz, K. W.; Kaufman, B. T.; Beddell, C. R.; Champness, J. N.; Stammers, D. K.; Kraut, J. *J. Biol. Chem.* **1985**, *260*, 381.
(12) Stammers, D. K.; Champness, J. N.; Beddell, C. R.; Dann, J. G.; Eliopoulos, E.; Geddes, A. J.; Ogg, D.; North, A. C. T. *FEBS Lett.* **1987**, *218*, 178.
(13) Champness, J. N.; Stammers, D. K.; Beddell, C. R. *FEBS Lett.* **1986**, *199*, 61.
(14) Oefner, C.; D'Arcy, A.; Winkler, F. K. *Eur. J. Biochem.* **1988**, *174*, 377.
(15) Li, R.-L.; Poe, M. *J. Med. Chem.* **1988**, *31*, 366.
(16) Selassie, C. D.; Fang, Z.-X.; Li, R. L.; Hansch, C.; Debnath, G.; Klein, T. E.; Langridge, R.; Kaufman, B. T. *J. Med. Chem.* **1989**, *32*, 1985.

0002-7863/91/1513-2295$02.50/0

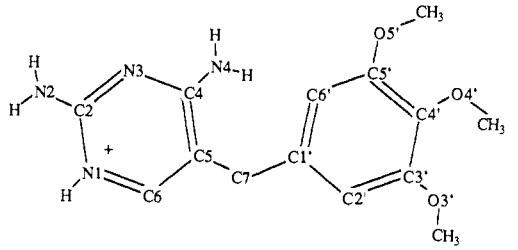

Figure 1. Structural formula for trimethoprim.

infections and cancer.[17,18] In addition, the ability of trimethoprim analogues to be strongly selective for the bacterial enzyme over the vertebrate analogue[19] will allow insights into the origin of specificity of these inhibitors to serve as a prototype for the development of general theoretical approaches to inhibitor design.

The calculation of the relative free energies of inhibitors binding to a common receptor has two major components, one of which is the solvation/desolvation thermodynamics of the drug, while the other is the thermodynamic cost of transforming one inhibitor into another in the enzyme-bound state.[5] Previous work performed by Brooks and Fleischman[9] has used free energy simulation methods to calculate the relative solvation thermodynamics for all combinations of 3′,4′,5′- and mono-, di-, and trisubstituted methoxy to ethyl substitutions on the benzyl ring of trimethoprim. From this work, an increased aqueous solubility for the 3′,5′-diethyl derivative relative to the trimethoxy benzyl derivative (over other diethyl compounds) was observed, similar to experimental measurements in which *p*-methoxy groups in substituted benzenes demonstrated enhanced hydrophilicity.[20] The origins of this effect, linked to entropic effects on solvation of the benzyl ring *p*-methoxy group, suggest that the thermodynamics of solvation/desolvation may contribute to the relative free energy of ligand binding to an enzyme. Similarly, consideration of the relative thermodynamics of transforming the enzyme-bound inhibitor from trimethoprim to the triethyl and *p*-ethyl derivatives and the determination of the relative free energies of binding have shown the importance of solvation/desolvation effects.[5] Although these results demonstrated the preference of the enzyme for the triethyl derivative over trimethoprim, in general agreement with experiment,[21,22] the major finding was that it is the favorable desolvation energy of the triethyl derivative relative to trimethoprim that confers most of the favorable relative binding energy of that derivative to the enzyme. The importance of both energetic and entropic factors in the binding process reinforces consideration of entropic factors in enzyme–ligand association.

In order to examine the criteria for enzyme–inhibitor specificity, the relative binding free energies for methoxy to ethyl substitutions at the 3′-, 4′-, and 5′-positions on the benzyl portion of the inhibitor were evaluated for mono-, di-, and trisubstituted derivatives (see Figure 1). The relative domination of energetic and entropic terms in the transformation of one species to another is discussed. Structural details of the transformed complexes are discussed with regard to enzyme–inhibitor interactions and comparison to crystallographic information on the chicken enzyme complex. The utility of predicting ligand–enzyme specificity via docking and energy minimization techniques is examined in light of modeling studies performed on the DHFR–inhibitor complexes.

Methods

A number of thermodynamic simulation studies have published detailed accounts of the background theory for these calculations. Therefore, we will not repeat them here. The reader is directed to the first paper in this series and references therein for additional background information on the details of the free energy methods.[9]

The inhibitors are transformed from one to another in terms of a reference and product state (A and B, respectfully), using a hybrid Hamiltonian defined in terms of a coupling parameter, λ, of the form $\mathcal{H}(\lambda) = (1 - \lambda)\mathcal{H}_A + \lambda\mathcal{H}_B + \mathcal{H}_{env}$, where λ = 0 equals state A, and λ = 1 equals state B. $\mathcal{H}_A$ corresponds to those atoms that are considered "reactant"; $\mathcal{H}_A$ are considered "product" atoms; $\mathcal{H}_{env}$ represents all solvent atoms (protein, cofactor, and water) and solute atoms chemically equivalent between states A and B. All inhibitor transformations used trimethoprim as the reference state.

The simulations were performed using a highly modified version of the CHARMM program running on a Cray Y-MP machine under the UNICOS operating system. The crystallographic structure of chicken dihydrofolate reductase, in complex with NADPH and trimethoprim, was used in all simulations.[11] Molecular dynamics simulations of the DHFR–NADPH–inhibitor–solvent complexes were carried out at four λ values to generate an ensemble of configurations for data reduction. The calculations used double-wide sampling at λ = (0.125, 0.5, 0.875, and 0.969), based upon a protocol developed in earlier calculations on this system,[5] with 7500 steps (11.25 ps) of equilibration and 30000 steps (45 ps) of production dynamics at each λ value. All simulations were carried out using the stochastic boundary molecular dynamics methodology[23,24] with 825 protein atoms, NADPH, inhibitor, and 61 TIP3P water molecules. A 14-Å reaction zone was used, centered at atom C7 of the inhibitor, with a 2-Å buffer region. The stochastic boundary region was prepared by first solvating and partially equilibrating solvent in a 14-Å reaction zone in the presence of a fixed protein and then equilibrating the entire system, with the atoms beyond 14 Å removed. The details of this procedure may be found in the appendix of ref 22. Solvent thermodynamics were computed by using three λ values (0.125, 0.5 and 0.875), with 20 ps of equilibration and 30 ps of production dynamics at each λ value. Additional sampling was performed for solvation thermodynamics at λ window 0.969 for the 4′-ethyl, 3′,4′-diethyl, and 3′,5′-diethyl congeners in order to assure a free energy convergence criteria of less than ca. 2 kcal/mol per λ value. The additional sampling proved unnecessary, however, since free energies computed with three windows gave similar results.[9] All calculations were done at 298 ± 5 K using Langevin dynamics for temperature control, by coupling all non-hydrogen atoms to the heat bath. Non-hydrogen buffer region atoms were constrained by harmonic forces derived from crystallographic temperature factors. All heteroatom–hydrogen bond lengths were constrained to equilibrium geometries by using the SHAKE algorithm.[25] A nonbonded cutoff of 8.5 Å was employed. Charges for the cofactor and inhibitors have been derived previously and are consistent with the CHARMM19 parameter set.[9,26] Force constants and nonbonded parameters for congeners of trimethoprim were taken from analogous fragments in the CHARMM parameter library.[27] The solvation thermodynamic simulations required to complete the binding cycle were computed as described in reference 9.

Results and Discussion

Thermodynamics of Inhibitor Binding. The relative free energy of inhibitor binding is evaluated from the following thermodynamic cycle:

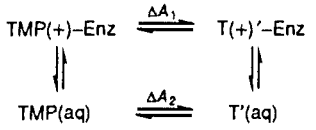

(1)

where TMP and T′ represent trimethoprim and the congener, TMP(+) and T(+)′ denote the protonated forms of the bound molecule, which is the relevant species when bound to DHFR as verified by NMR,[28-30] aq denotes the calculation in an aqueous

(17) Hitchings, G. H.; Roth, B. In *Enzyme Inhibitors as Drugs*; Sandler, M., Ed.; Macmillan: New York, 1980; pp 263–280.
(18) Hitchings, G. H. *Agnew. Chem., Int. Ed. Engl.* **1989**, *28*, 879.
(19) Baccanari, D. P.; Daluge, S.; King, R. W. *Biochemistry* **1982**, *21*, 5068.
(20) Anderson, G. M.; Kollman, P. A.; Domelsmith, L. N.; Houk, K. N. *J. Am. Chem. Soc.* **1979**, *101*, 2344.
(21) Matthews, D. A.; Bolin, J. T.; Burridge, J. M.; Filman, D.; Volz, D. J.; Kaufman, B. T.; Beddell, C. R.; Champness, J. M.; Stammers, D. K.; Kraut, J. *J. Biol. Chem.* **1985**, *260*, 392.
(22) Roth, B.; Aig, E. *J. Med. Chem.* **1987**, *30*, 1998.
(23) Brooks, C. L.; Karplus, M. *J. Mol. Biol.* **1989**, *208*, 159.
(24) Brooks, C. L.; Brunger, A.; Karplus, M. *Biopolymers* **1985**, *24*, 843.
(25) Ryckaert, J.-P.; Ciccotti, G.; Berendsen, H. J. C. *J. Comput. Phys.* **1977**, *23*, 327.
(26) Brooks, B. R.; Bruccoleri, R. E.; Olafson, B. D.; States, D. J.; Swaminathan, S.; Karplus, M. *J. Comput. Chem.* **1983**, *4*, 187.
(27) Parameters for trimethoprim analogues and NADPH are available from the authors upon request.
(28) Bevan, A. W.; Roberts, G. C. K.; Feeney, J.; Kuyper, L. *Eur. J. Biophys.* **1985**, *11*, 211.
(29) Roberts, G. C. K.; Feeney, J.; Burgen, A. S. V.; Daluge, S. *FEBS Lett.* **1981**, *131*, 85.

Table I. Thermodynamics of Inhibitor Binding Relative to Trimethoprim (kcal/mol)

inhibitor	transformation type	$\Delta\Delta A$	$\Delta\Delta E$	$T\Delta\Delta S$
3′-ethyl	(solv)[a]	−1.5 ± 0.2	−12.4 ± 5	−10.9 ± 5
	(Enz)[b]	−4.3 ± 0.2	−8.5 ± 6	−4.2 ± 6
	(Enz)−(solv)	−2.8 ± 0.3	3.9 ± 7	6.7 ± 7
4′-ethyl	(solv)[a]	−1.5 ± 0.2	−16.5 ± 5	−15.0 ± 5
	(Enz)[b]	−1.1 ± 0.2	6.6 ± 7	7.7 ± 5
	(Enz)−(solv)	0.4 ± 0.3	23.1 ± 8	22.7 ± 8
5′-ethyl	(solv)[a]	−1.5 ± 0.1	−12.4 ± 5	−10.9 ± 5
	(Enz)[b]	−1.1 ± 0.3	−16.7 ± 9	−15.6 ± 9
	(Enz)−(solv)	0.4 ± 0.3	−4.3 ± 10	−4.7 ± 10
3′,4′-diethyl	(solv)[a]	−2.4 ± 0.2	−18.6 ± 7	−16.2 ± 7
	(Enz)[b]	−3.2 ± 0.4	−8.9 ± 8	−5.8 ± 8
	(Enz)−(solv)	−0.8 ± 0.5	9.7 ± 10	10.4 ± 10
4′,5′-diethyl	(solv)[a]	−2.4 ± 0.2	−18.6 ± 7	−16.2 ± 7
	(Enz)[b]	−5.0 ± 0.3	−3.7 ± 8	1.3 ± 8
	(Enz)−(solv)	−2.6 ± 0.4	14.9 ± 11	17.5 ± 11
3′,5′-diethyl	(solv)[a]	−2.1 ± 0.2	4.1 ± 6	6.2 ± 6
	(Enz)[b]	−4.3 ± 0.3	15.3 ± 10	19.6 ± 10
	(Enz)−(solv)	−2.2 ± 0.4	11.2 ± 12	13.4 ± 12
3′,4′,5′-triethyl	(solv)[a]	−4.9 ± 0.3	−2.7 ± 6	2.2 ± 6
	(Enz)[b]	−6.3 ± 0.3	−9.0 ± 8	−2.7 ± 8
	(Enz)−(solv)	−1.4 ± 0.5	−6.3 ± 10	−4.9 ± 10

[a] Corresponds to $\Delta\Delta A_2$ from eq 1. [b] Corresponds to ΔA_1 from eq 1.

environment, and T(+)′-Enz represents the trimethoprim congener in the bound environment of the protein. The relative free energy of binding is equal to ΔA_1 (the protein part) − ΔA_2 (the aqueous part). The relative free energies for inhibitor binding, along with the component thermodynamics for the solvated and protein-bound inhibitors, are shown in Table I. The statistical precision of these values, also listed in this table, has been estimated as the standard deviation of bin averages.[31] The uncertainties for $\Delta\Delta E$ and $\Delta\Delta S$ are large owing to their origin from the derivatives of the free energy. However, previous work has demonstrated the statistical significance of the difference between the entropic and energetic components.[5] thereby allowing the discussion of the relative importance of these components. The reliability of the free energy differences obtained from this methodology, as noted by Fleischman and Brooks,[5] has been shown to be within a few tenths of a kilocalorie per mole, based upon thermodynamic simulations that were repeated from different initial velocity and starting configuration conditions.

The trend for the calculated relative affinity of the inhibitors for the enzyme follows the ordering 3′-ethyl > 4′,5′-diethyl > 3′,5′-diethyl > 3′,4′,5′-triethyl > 3′,4′-diethyl > trimethoprim > 5′-ethyl > 4′-ethyl. Of course, the 3′,4′-diethyl and 4′,5′-diethyl derivatives are indistinguishable, as are 5′-ethyl and 3′-ethyl derivatives, regarding their observable binding to DHFR. However, these calculations reflect local or intrinsic binding thermodynamics and indicate that symmetry-related inhibitors respond differently to the asymmetric binding pocket. Figure 2 graphically illustrates the relative binding thermodynamics of the trimethoprim congeners. Figure 3 illustrates the different environments of the 5′-group, near Tyr31, and the 3′-group, near Val115.

The approximate ordering of two of these derivatives has been confirmed experimentally. As discussed in initial work by Fleischman and Brooks, the triethyl derivative is shown to bind 1.4 kcal/mol more tightly to the enzyme than does trimethoprim,[5] in good agreement with an experimental value of approximately 1.7 kcal/mol.[21,22] Similar experiments on the homologous rat liver enzyme have shown an increased affinity for the 3′,5′-diethyl analogue of trimethoprim.[32,33] This is indicated from our calculations. However, small differences in inhibitor affinities between the two vertebrate enzymes make it impossible to rate the relative affinity of the 3′,5′-diethyl analogue relative to the triethyl derivative.

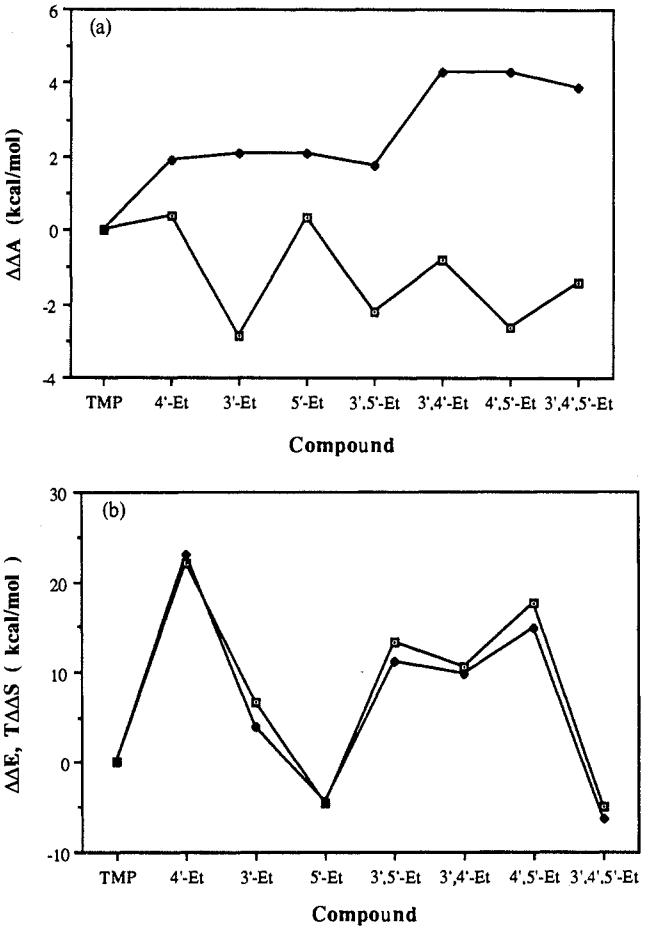

Figure 2. Relative binding thermodynamics for trimethoprim: (a) free energy of binding ($\Delta\Delta A_{bind}$) relative to trimethoprim. (b) energy ($\Delta\Delta E_{bind}$) and entropy ($\Delta\Delta S_{bind}$) of binding relative to trimethoprim. Closed diamonds denote the solvation thermodynamics of the inhibitors and open squares denote the relative binding thermodynamics.

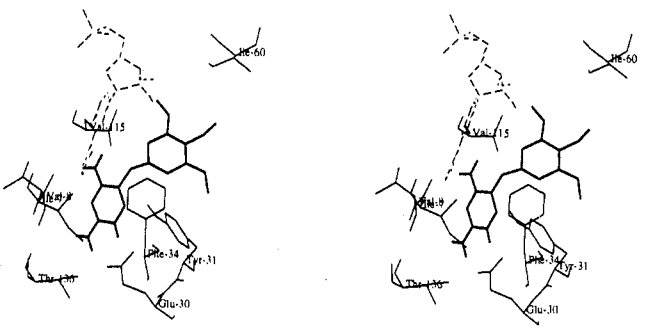

Figure 3. Stereodiagram of stochastic boundary region for the DHFR–solvent–inhibitor–NADPH complex employed in thermodynamic simulations. Trimethoprim is identified by heavy lines. NADPH is shown with dashed lines.

A comparison of the relative differences in energetic and entropic components between congeners can be understood in terms of the closed thermodynamic cycle:

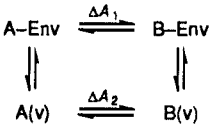

(2)

where A–Env and B–Env represent the initial and final states of the inhibitor, and Env indicates the presence of the solvated protein

(30) Cocco, L.; Roth, B.; Temple, C.; Montgomery, J. A.; London, R. E.; Blakley, R. L. *Arch. Biochem. Biophys.* **1983**, *226*, 567.
(31) Schiferel, S. K.; Wallace, D. C. *J. Chem. Phys.* **1985**, *83*, 5203.
(32) Roth, B.; Rauckman, B. S.; Ferone, R.; Baccanari, D. P.; Champness, J. N.; Hyde, R. M. *J. Med. Chem.* **1987**, *30*, 348.
(33) Roth, B.; Aig, E.; Lance, K.; Rauckman, B. S. *J. Med. Chem.* **1980**, *23*, 535.

Table II. Protein/Cofactor Environment and Solvation Contributions to Relative Free Energies of Inhibitor Binding (kcal/mol)

inhibitor	transformation type	$\Delta\Delta A$		$\Delta\Delta E$		$T\Delta\Delta S$	
		protein	solvent[a]	protein	solvent	protein	solvent
3′-ethyl	(v)[b]	−3.5 ± 0.2		−2.9 ± 4		0.6 ± 4	
	(Env)[c]	−4.3 ± 0.2		−8.5 ± 6		−4.2 ± 6	
	(Env)−(v)	−0.8 ± 0.2	2.0 ± 0.2	−5.6 ± 7	−9.5 ± 6	−4.8 ± 7	−11.5 ± 6
4′-ethyl	(v)[b]	−3.4 ± 0.1		−5.2 ± 2		−1.8 ± 2	
	(Env)[a]	−1.1 ± 0.2		6.6 ± 7		7.7 ± 5	
	(Env)−(v)	2.3 ± 0.3	1.9 ± 0.2	11.8 ± 7	−11.3 ± 5	9.5 ± 5	−13.2 ± 5
5′-ethyl	(v)[b]	−3.5 ± 0.2		−2.9 ± 4		0.6 ± 4	
	(Env)[c]	−1.1 ± 0.3		−16.7 ± 9		−15.6 ± 9	
	(Env)−(v)	2.4 ± 0.4	2.0 ± 0.2	−13.8 ± 10	−9.5 ± 6	−16.2 ± 10	−11.5 ± 6
3′,4′-diethyl	(v)[b]	−6.7 ± 0.4		−6.8 ± 9		−0.1 ± 9	
	(Env)[c]	−3.2 ± 0.4		−8.9 ± 8		−5.8 ± 8	
	(Env)−(v)	3.5 ± 0.6	4.3 ± 0.4	−2.1 ± 12	−11.8 ± 11	−5.7 ± 12	−16.1 ± 11
4′,5′-diethyl	(v)[b]	−6.7 ± 0.4		−6.8 ± 9		−0.1 ± 9	
	(Env)[a]	−5.0 ± 0.3		−3.7 ± 8		1.3 ± 11	
	(Env)−(v)	1.7 ± 0.5	4.3 ± 0.4	3.1 ± 12	−11.8 ± 11	1.4 ± 14	−16.1 ± 11
3′,5′-diethyl	(v)[b]	−3.9 ± 0.2		−4.3 ± 4		−0.5 ± 4	
	(Env)[c]	−4.3 ± 0.3		15.3 ± 8		19.6 ± 10	
	(Env)−(v)	−0.4 ± 0.4	1.8 ± 0.3	19.6 ± 9	8.4 ± 7	20.1 ± 11	6.6 ± 7
3′,4′,5′-triethyl	(v)[b]	−8.8 ± 0.4		−6.8 ± 9		2.0 ± 9	
	(Env)[c]	−6.3 ± 0.5		−9.0 ± 8		−2.7 ± 10	
	(Env)−(v)	2.5 ± 0.6	3.9 ± 0.5	−2.2 ± 12	4.1 ± 11	−4.7 ± 13	0.2 ± 11

[a] Data taken from ref 9. [b] Corresponds to ΔA_2 from eq 2. [c] Corresponds to ΔA_1 from eq 2. Env for protein is protein–solvent–cofactor. Env for solvent is bulk water.

environment (as in ΔA_1 from eq 1), or the presence of bulk solvent (as in ΔA_2 from eq 1). This thermodynamic cycle represents the thermodynamic cost of transforming inhibitor A to B in vacuo. The difference of $\Delta A_1 - \Delta A_2$, from eq 2, yields the relative component thermodynamic contributions of the environment to inhibitor transformation. Where Brooks and Fleischman have used bulk solvent as Env to report the relative free energies of solvation for these inhibitors, this study uses the solvated protein as Env to report the thermodynamic contribution of the protein environment to inhibitor transformation. The components energy values are tabulated in Table II.

A clear difference in the relative free energy of binding for the trimethoprim 3′- and 5′-congeners is illustrated in Figure 2. The thermodynamic cost of transforming either of these inhibitors in solvent or in vacuum is the same because the two compounds are related by symmetry. Therefore, the difference in binding free energy is associated with the transformation in the bound enzyme state. Table II illustrates that the 5′-derivative is favored energetically over the 3′-derivative. Both transformations are disfavored entropically. However, the 3′-derivative is disfavored less, weighting the preference for the 3′-derivative over the 5′-derivative. In addition, it is interesting to note the addition of the ethyl moiety in the region of the tyrosine side chain at position 31 produces much lower energetic and entropic effects, arising from the protein environment contribution to the free energy.

The transformation of trimethoprim to the 4′-methoxy species produces thermodynamics different from the 3′- or 5′-derivative. While the free energy of solvation for the 4′-methoxy derivative follows the same trends as the other monosubstituted species, the enzyme-bound inhibitor shows very different behavior (Table II). Both the 3′- and 5′-ethyl derivatives demonstrate favorable energetic and disfavorable entropic contributions. However, the 4′-ethyl derivative shows quite the opposite behavior with a marked disfavorable energetic component and a favorable entropic one.

The thermodynamics of the symmetrically related 3′,4′- and 4′,5′-diethyl derivatives may be compared by using the differences in the protein-bound transformations alone, using the same argument as for the 3′- and 5′-species. The 3′,4′-diethyl derivative is favored energetically over the 4′,5′-diethyl derivative by approximately 5 kcal/mol. However, the 3′,4′-diethyl derivative is disfavored entropically over the 4′,5′-diethyl derivative by approximately 7 kcal/mol, weighting the preference for the 4′,5′-diethyl derivative.

The thermodynamics for the 3′,5′-diethyl derivative are different from the other disubstituted derivatives in terms of both the solvation thermodynamics, as indicated in the introduction, and the enzyme-bound thermodynamics. The protein environment thermodynamics for 3′,4′- and 4′,5′-diethyl derivatives each have energetic or entropic changes that are of small magnitude (Table II). However, the 3′,5′-diethyl derivative possesses large magnitude changes for both, resulting in a marginally favorable relative free energy from the protein environment. Together with the favorable desolvation free energy, the 3′,5′-diethyl derivative is both predicted and observed to bind more favorably to the enzyme than trimethoprim.

The 3′,4′,5′-triethyl derivative is shown to have the most favorable desolvation free energy relative to trimethoprim (−3.9 kcal/mol),[9] arising from the transformation of three methoxy groups to ethyl groups. The free energy contribution from the protein environment (2.5 kcal/mol: from Table II) is slightly unfavored, resulting mostly from an unfavorable entropic contribution. However, the overall relative binding free energy is favorable (−1.4 kcal/mol), with most of the driving force arising from a favorable energetic component (−6.3 kcal/mol from Table II).

A noted feature of the relative binding free energies (Figure 2), related to the preference of the enzyme for 3′- or 5′-based derivatives, is the reversal of the preferences depending on whether the inhibitor is mono- or disubstituted. The 3′-methoxy derivative is preferred over the 5′-derivative by 3.2 kcal/mol, while the 4′,5′-dimethoxy derivative is preferred over the 3′,4′-dimethoxy derivative by 1.8 kcal/mol. The presence of the additional 4′-ethyl group in the disubstituted species does not contribute equally to the thermodynamics in the 3′,4′- and 4′,5′-diethyl derivatives. To understand the origins of these differences, it is necessary to compare the different thermodynamic contributions from protein and solvent in the following four pairs of inhibitor systems: 3′-ethyl/5′-ethyl, 3′,4′-diethyl/4′,5′-diethyl, 3′-ethyl/3′,4′-diethyl, and 5′-ethyl/4′,5′-diethyl.

As stated above, the 3′- and 5′-ethyl derivatives differ thermodynamically. The energetic contribution for the 3′-ethyl derivative is dominated by an unfavorable solvation term (See Table II), while the 5′-ethyl derivative is dominated by a favorable protein contribution. The entropic contribution to the 3′-ethyl derivative is dominated by a favorable entropic solvation term, while the 5′-ethyl derivative is dominated by an unfavorable protein term. The relative free energy of the 3′-ethyl derivative is dominated by a favorable solvation component, while the 5′-ethyl derivative is dominated by an unfavorable protein contribution.

The 3′,4′- and 4′,5′-diethyl derivatives, though different in the magnitude of their thermodynamic components, possess similar trends in their relative thermodynamics. The energetic contri-

Table III. Coordinate Root Mean Square Differences between Models[a] and Crystal Structure of DHFR-NADPH-Inhibitor Complex (Angstroms)

	atom types[b]		
system	all[c] (677)	backbone (332)	neighbors[d] (57)
trimethoprim	1.4	0.90	0.65
3′-ethyl	1.5	0.86	0.88
4′-ethyl	1.6	0.96	0.70
5′-ethyl	1.6	0.94	0.69
3′,4′-diethyl	1.6	0.96	0.57
3′,5′-diethyl	1.5	1.00	0.63
4′,5′-diethyl	1.4	0.88	0.65
3′,4′,5′-triethyl	1.6	1.00	0.72

[a] Models obtained from averaging 250 coordinate sets, representing 7500 steps of SBMD, followed by energy minimization. [b] Data sets taken from set of all non-hydrogen protein and NADPH atoms found in the SBMD region. [c] Number of atoms compared. [d] Neighbors include all atoms within 3.5 Å of the inhibitor molecule.

butions of both are dominated by an unfavorable solvation component. In addition, the entropic contributions are dominated by a favorable solvation component. The relative free energies of both are dominated by a favorable solvation component. The 3′-ethyl and 3′,4′-diethyl derivatives also possess similar trends in their overall relative thermodynamics. In both, the overall relative free energies are dominated by a favorable solvation component. In addition, the energetic and entropic contributions are similar. Both the 3′-ethyl and 3′,4′-diethyl derivatives are dominated by an unfavorable solvation component to energy, and a favorable solvation component to entropy. An identical trend is observed in the comparison of the 3′,4′- and 4′,5′-diethyl derivatives.

While the 5′-ethyl derivative is dominated by a favorable protein contribution to the energetic component, the 4′,5′-diethyl derivative is dominated by an unfavorable solvation contribution to the energetic component. This reversal is also noted for the entropic component, where the 5′-ethyl derivative is dominated by an unfavorable protein contribution and the 4′,5′-diethyl derivative is dominated by a favorable solvation contribution. The overall effect on the free energy makes the 5′-ethyl derivative dominated by an unfavorable protein component to the free energy, while the 4′,5′-diethyl derivative is dominated by a favorable solvation component. It is this difference in the apparent thermodynamic trends between the 5′-ethyl and 4′,5′-diethyl derivatives that accounts for the reversal in binding trends. These results indicate that the presence of the 4′-ethyl group does not affect the thermodynamics in a similar manner for the 3′,4′- and 4′,5′-diethyl derivatives, but rather influences neighboring active site atoms differently, causing changes in the relative thermodynamics.

Structural Evaluation of the Inhibitor-Enzyme Complexes. The structural evaluation of inhibitor-DHFR-NADPH-solvent complexes was made by using two techniques. In the first, a set of coordinates was obtained from averaging and minimizing an ensemble of 250 coordinate sets generated from 7500 steps of stochastic boundary molecular dynamics (SBMD) performed at the end-point states of the thermodynamic perturbation calculations. These coordinate sets were used to report root mean square differences relative to the crystal structure and identify protein-inhibitor contacts and inhibitor interaction energies. In the second, this same ensemble of configurations was used to construct time series of physical properties, including inhibitor dihedral angle fluctuations and inhibitor interaction energies, from which mean and standard deviation information was derived.

A comparison of each of the structures with the crystal structure reveals a general preservation of structure both in the protein and in the placement and conformation of the inhibitor. Coordinate root mean square differences for the protein and heteroatoms used in the calculation were compared against equivalent atoms in the crystal structure. The results are shown in Table III. The preservation of structure is particularly evident in the neighbors column, which reports the fit over all protein and NADPH heteroatoms within 3.5 Å of any inhibitor atoms.

Table IV identifies the hydrogen bonds at the pyrimidine portion of the inhibitor and the neighbor contacts found at the substituent positions of the benzyl ring. The pyrimidine portion consistently makes the same contacts with the protein for the different inhibitors. The only exceptions are the structures from the 3′,4′,5′-triethyl and 3′,5′-diethyl derivatives, which do not make contact with the Val115 residue. Time series analysis of the stored coordinate sets from the end-point MD trajectories also shows the absence of any hydrogen bonding between these atoms. The hydrogen bond between the carbonyl group of Val115 and the inhibitor's 4-amino group has been implicated in conferring the specificity of inhibitor binding for the bacterial over the vertebrate enzyme.[11] The absence of any correlation between the loss of the hydrogen bond and the relative free energies of binding tends to support a lesser role for this hydrogen bond.

The ϕ_1/ϕ_2 dihedral angles of trimethoprim, defined by the C1′-C7 and C7-C5 bonds, respectively, define the conformation of the trimethoprim molecule. Because the pyrimidine is found

Table IV. Contacts and Neighbors[a] Observed between Inhibitor and Protein/Cofactor in Dynamics Averaged Structures

	benzyl contacts/neighbors[b,c]			pyrimidine hydrogen bonds		
system	3′	4′	5′	N1	N2	N4
trimethoprim			Tyr31 (2)	Glu30 Solv	Glu30	Ile7 Val115
3′-ethyl	Ile60 (1) Phe34 (1)	Val112 (1)	Tyr31 (3) Phe34 (1)	Glu30 Solv	Glu30 Thr136	Ile7 Val115
4′-ethyl	Val115 (1)		Tyr31 (3)	Glu30 Solv	Val8 Glu30 Thr136	Ile& Val115
5′-ethyl	Phe34 (1)			Glu30 Solv	Val8 Glu30	Ile7 Val115
3′,4′-diethyl	Val115 (1) Phe34 (1)			Glu30 Solv	Val8 Glu30 Val136	Ile7 Val15
4′,5′-diethyl	Val115 (2) Phe34 (1)		Tyr31 (1)	Glu30 Solv	Val8 Thr136 Solv	Ile7 Val115
3′,5′-diethyl	Val115 (1)	Phe34 (1)	Tyr31 (1)	Glu30 Solv	Val8 Glu30 Thr136	Ile7
3′,4′,5′-triethyl	Phe34 (1) Val115 (1)	Nic(1)[d]		Glu30 Solv	Val8 Glu30 Thr136	Ile7

[a] Neighbors are defined as all atoms within 3.5 Å of any inhibitor atom. [b] Contacts or neighbors to the 3′, 4′, or 5′ functional groups in the benzyl portion of the inhibitor. [c] Numbers in parentheses indicate the number of contacts or neighbors for a given residue. [d] Nic denotes the nicotinamide portion of NADPH.

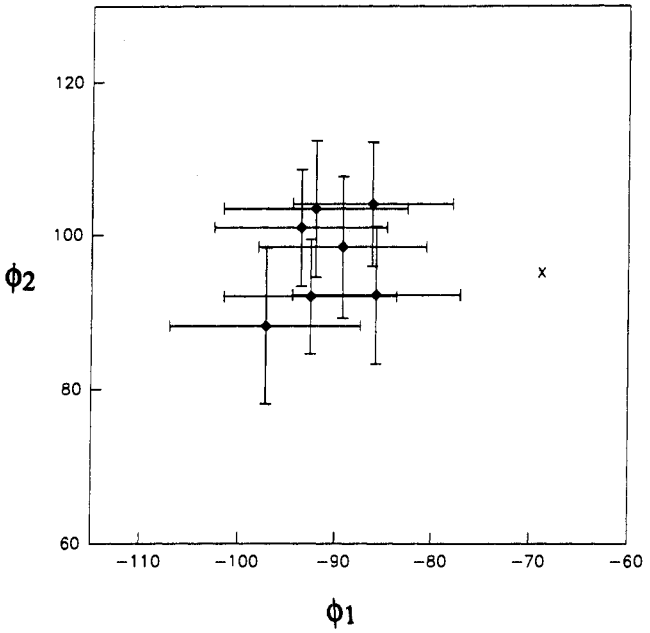

Figure 4. Plot of ϕ_1 (C1′–C7) and ϕ_2 (C7–C5) dihedral angles found in trimethoprim. Diamonds (with error bars) denote the mean and standard deviation angles for the seven substituted inhibitor derivatives derived from molecular dynamics. X marks the dihedral angles found in the chicken DHFR ternary complex crystal structure.

to consistently maintain the same contacts, dihedral angle changes tend to reflect slight changes in the attitude of the benzyl ring of the inhibitor. Figure 4 illustrates the mean and standard deviation of these dihedral angles taken from the end-point trajectories. The X indicates the dihedral angle values for the bound trimethoprim conformation in the crystal structure form of the chicken DHFR enzyme. While the mean of the ϕ_2 angles is centered at approximately the same position as the crystal structure, a systematic bias appears to be present for the ϕ_1 dihedral angles. These slightly more negative values are consistent with the inhibitor obtaining a slightly more stacked planar arrangement with the phenyl ring of Phe-34 in the enzyme, presumably maximizing van der Waals contacts, and may be a slight artifact of the potentials used in the present calculations.[34]

The question of choosing computationally less expensive techniques for evaluating the relative affinities of ligands for proteins is an important one. In this work, we have examined the utility of molecular dynamics derived potential energies of protein–drug interaction to predict the relative affinities of the inhibitors for the chicken DHFR enzyme. Two techniques were employed, similar to those for the structural evaluations of the complexes. From the averaged/minimized structures, as described above, potential energies were derived for interactions between inhibitor/water, inhibitor/protein, and inhibitor/environment. Environment includes protein, water, and cofactor. These are tabulated in Table V. Potential energies were also derived for the time series of coordinate sets from the end-point MD trajectories. The various potential energies of interaction, shown in Table VI, represent the mean interaction energies and standard deviations from the mean.

The relative free energies of inhibitor binding, shown in Table I, use trimethoprim as the reference state. To obtain a similar accounting of the relative potential energies, the interaction energy of trimethoprim was subtracted from the interaction energies of the other inhibitor–enzyme complexes. The results are shown in Table VII. The results indicate that four out of seven complexes clearly do not follow the same trends as the relative free energies (e.g., 3′,4′-diethyl, 4′,5′-diethyl, 3′,5′-diethyl, 3′,4′,5′-triethyl). The three others, 4′-ethyl, 3′-ethyl, and 5′-ethyl, have values quite

(34) Burley, S. K.; Petsko, G. A. *Science* **1985**, *229*, 23.

Table V. Inhibitor Interaction Energies from Dynamics Averaged and Energy Minimized Coordinate Sets (kcal/mol)

	atoms evaluated		
system	protein[a] and water	protein[a]	water
trimethoprim	−155.7	−136.0	−17.7
3′-ethyl	−158.9	−149.6	−8.3
4′-ethyl	−155.5	−142.0	−13.5
5′-ethyl	−155.1	−139.7	−15.4
3′,4′-diethyl	−151.1	−133.6	−17.5
4′,5′-diethyl	−155.2	−129.2	−25.3
3′,5′-diethyl	−145.5	−131.1	−14.4
3′,4′,5′-triethyl	−144.3	−133.0	−11.3

[a] Protein includes all protein and cofactor atoms.

similar to the free energies. However, some doubt is cast on these three given that two of the three (i.e., 3′-ethyl and 5′-ethyl derivatives) are dominated by the entropic term in the relative free energies, a parameter for which the interaction energies cannot account.

If the overall energetics are unrelated to the relative free energies, are there any general trends that can be derived from the interaction energies? Without regard to the free energy results, the trends observed from the interaction energies alone would implicate the trimethoprim complex to be the most favorable. Time series analysis shows that the trimethoprim complex produces the least favorable pyrimidine–water dynamics interactions. This may be due, in part, to fewer waters in the active site. However, benzyl–water interactions for trimethoprim are better than any other inhibitor complex, and this is to be anticipated because of the presence of the three methoxy groups in this case. Time series analysis shows the pyrimidine–protein interactions to be among the most favorable, perhaps in compensation for the absence of favorable pyrimidine–water interactions. Benzyl–protein interactions are among the least favorable, in part due to the more favorable benzyl–water interactions. Data from both time series and average/minimized structures indicate the overall inhibitor–water interaction for trimethoprim to be among the most favorable. Time series of the inhibitor–protein and inhibitor–environment interactions show the trimethoprim model to be favored overall. Similarly, the averaged/minimized models would predict trimethoprim to be the second most favored, behind the 3′-ethyl derivative by 3.2 kcal/mol.

The energy-based techniques appear to produce results that are neither consistent with each other nor able to reproduce the trend of experimental results. No observable trends were found that correlate interaction energies to the computed relative binding free energies, or the thermodynamic contribution of protein environment to the free energies (Table II). These results indicate interaction energies alone may be insufficient to determine the relative affinities of a ligand for a protein, particularly for small molecules where desolvation may be a crucial component.

Summary

This paper reports the work of thermodynamic simulation studies for the determination of the relative free energies of inhibitor binding by chicken dihydrofolate reductase. In an effort to search for computationally less intensive means of predicting the relative affinities of drugs for a receptor, the thermodynamic results have also been compared to potential energies between inhibitor and enzyme, as derived from MD simulations.

The results of the thermodynamic calculations for two of the derivatives (i.e., 3′,5′-diethyl and 3′,4′,5′-triethyl) corroborate experimental findings regarding the affinities of the inhibitors relative to trimethoprim. No experimental information is available for the other derivatives examined. While the predicative ability of free energy simulation techniques is encouraging, this study was unable to demonstrate a trend with regard to a benzyl position that, when modified, consistently affects the relatively free energy in a predicted fashion. In fact, quite the opposite was observed. The thermodynamic effects of a substitution or group of substitutions are greatly affected by neighboring inhibitor atoms, and the influences such neighbors have on the local environment of

Table VI. Inhibitor Interaction Energies from Time Series Averages (kcal/mol)[a]

system	sets of interactions evaluated						
	pyr-protein	benzyl-protein	pyr-water	benzyl-water	inh-protein	inh-water	inh-all
trimethoprim	-110.8 ± 4.5	-17.6 ± 1.8	1.2 ± 3.6	-16.0 ± 2.3	-129.9 ± 4.7	-15.1 ± 4.2	-145.1 ± 6.1
3'-ethyl	-104.3 ± 4.4	-22.6 ± 1.7	-5.2 ± 4.7	-5.0 ± 2.0	-127.6 ± 4.2	-11.9 ± 5.0	-139.5 ± 5.6
4'-ethyl	-109.2 ± 4.2	-19.8 ± 1.9	-3.6 ± 2.9	-8.5 ± 1.9	-129.6 ± 5.0	-12.3 ± 3.7	-141.9 ± 5.3
5'-ethyl	-109.3 ± 3.9	-19.0 ± 1.8	-2.8 ± 3.8	-9.0 ± 2.2	-128.8 ± 4.2	-12.0 ± 4.8	-140.7 ± 5.6
3',4'-ethyl	-99.9 ± 4.7	-18.7 ± 2.0	-5.3 ± 3.7	-10.9 ± 1.9	-120.2 ± 5.4	-16.4 ± 4.4	-136.6 ± 6.4
4',5'-ethyl	-101.3 - 4.1	-18.4 ± 1.6	-8.3 ± 4.7	-8.8 ± 2.1	-120.3 ± 4.3	-17.3 ± 5.1	-137.6 ± 5.8
3',5'-diethyl	-102.4 ± 4.5	-18.3 ± 1.5	-4.1 ± 3.8	-6.2 ± 2.0	-121.3 ± 4.5	-10.5 ± 4.2	-131.8 ± 5.7
3',4',5'-triethyl	-99.4 ± 4.6	-18.2 ± 1.4	-5.0 ± 1.4	-14.8 ± 2.5	-119.5 ± 4.9	-20.1 ± 5.5	-139.7 ± 5.6

[a] Pyr corresponds to pyrimidine portion of the inhibitor. Protein includes all protein and cofactor atoms. Benzyl refers to the benzyl portion of inhibitor. Inhibitor includes all inhibitor atoms.

Table VII. Comparison of Potential Energy of Inhibitor-Protein Interaction and Relative Free Energies of Binding (kcal/mol)

source of data set	model complex	inhib interactn energies	rel interactn energies[a]	rel free energies[b]
averaged, minimized	3'-ethyl	-158.9	-3.2	-2.8
	4'-ethyl	-155.5	0.2	0.4
	5'-ethyl	-155.1	0.6	0.4
	3',4'-diethyl	-151.1	4.6	-0.8
	4',5'-diethyl	-155.2	0.5	-2.7
	3',5'-diethyl	-145.5	10.2	-2.2
	3',4',5'-triethyl	-144.3	11.4	-1.4
time series averages	3'-ethyl	-139.5	5.6	-2.8
	4'-ethyl	-141.9	3.2	0.4
	5'-ethyl	-140.7	4.4	0.4
	3',4'-diethyl	-136.6	8.5	-0.8
	4',5'-diethyl	-137.6	7.5	-2.7
	3',5'-diethyl	-131.8	13.3	-2.2
	3',4',5'-triethyl	-139.7	5.4	-1.4

[a] Relative interaction energies were obtained by calculating the difference in interaction energy relative to the trimethoprim complex. Interaction energies for the reference complex were -155.7 kcal/mol for the averaged, minimized structure and -145.1 kcal/mol for the time series average. [b] Taken from Table I.

the enzyme active site and solvation thermodynamics. A case in point is the reversal of the preference of the enzyme for ethylation of the 3'- or 5'-position, depending on the presence or absence of the 4'-ethyl group. We observed the 3'-ethyl derivative to be preferred over the 5'-ethyl derivative. However, the opposite trend was observed for the disubstituted 3',4'- and 4',5'-diethyl derivatives. While the 3'-ethyl and 3',4'-diethyl derivatives demonstrated similar trends in terms of the contribution of protein or solvation components to the thermodynamics, the 5'-ethyl and 4',5'-diethyl derivatives exhibited different thermodynamics, both in terms of the relative dominance of energetic and entropic components and the thermodynamic contribution from protein or solvent. The results appear to demonstrate a complex relationship between the contribution of protein and solvent effects to the thermodynamics of the inhibitor binding. Energetic analysis alone, by calculating the potential energies of inhibitor interaction with its environment, did not correlate with the relative thermodynamics calculations by the free energy simulation technique.

The models of the complexes obtained after averaging the coordinates over MD simulations at the thermodynamic end points, and energy minimizing to remove short contacts, revealed very few structural differences with reference to the crystal structure or each other. One feature of note, however, was the observation of hydrogen bonds between the carbonyl oxygen of Val115 and the N4 group in the inhibitor pyrimidine ring in six of eight complexes. The presence of this hydrogen bond in the *Escherichia coli* species of the enzyme and its absence in the vertebrate species has been linked to the source of inhibitor specificity for the bacterial enzyme. However, no correlation was observed between the existence of this hydrogen bond and the relative free energies of inhibitor binding, leading us to speculate about a reduced importance of this interaction in conferring stability to the bacterial species. The results of similar inhibitor transformations on the bacterial enzyme will be reported shortly.

Acknowledgment. Support from the NIH (Grant 37554) is gratefully acknowledged. C.L.B. is an Alfred P. Sloan Research Fellow. This research was supported in part by a grant from the Pittsburgh Supercomputing Center through the NIH Division of Research Resources Cooperative Agreement U41RR04154 and through a grant from the National Science Foundation, Cooperative Agreement ASC-8500650.

Registry No. DHFR, 9002-03-3; trimethoprim, 738-70-5; 3'-ethyltrimethoprim, 131618-99-0; 4'-ethyltrimethoprim, 78026-01-4; 3',4'-diethyltrimethoprim, 131619-00-6; 3',5'-diethyltrimethoprim, 36821-88-2; 3',4',5'-triethyltrimethoprim, 36821-85-9.

Communications to the Editor

The Condensation of Dicarbonyl Compounds with *N*-Phenyltriazolinedione-Dienone Ylides Derived from Phenols: The Facile Preparation of Novel Quinone Methides

R. Marshall Wilson* and Nuanphun Chantarasiri

Department of Chemistry, University of Cincinnati Cincinnati, Ohio 45221-0172

Received July 23, 1990
. Revised Manuscript Received December 31, 1990

Alkylated urazoles have been observed to undergo oxidation to *N*-phenyltriazolinedione (PTAD) ylides and these ylides to serve as highly activated carbonyl equivalents in condensations with enolates and other nucleophiles.[1] In addition, *N*-phenyltriazolinedione is known to add to a variety of aromatic molecules to form the corresponding arylated urazoles (Scheme I).[2,3]

(1) (a) Wilson, R. M.; Hengge, A. C. *Tetrahedron Lett.* **1985**, *26*, 3673. (b) Wilson, R. M.; Hengge, A. *J. Org. Chem.* **1987**, *52*, 2699. (c) Wilson, R. M.; Hengge, A. C. *J. Org. Chem.* **1990**, *55*, 197. (d) Wilson, R. M.; Hengge, A. C.; Ataei, A.; Ho, D. M. *J. Am. Chem. Soc.*, in press.

(2) (a) Wamhoff, H.; Wald, K. *Chem. Ber.* **1977**, *110*, 1699. (b) Hall, J. H. *J. Org. Chem.* **1983**, *48*, 1708. (c) Hall, J. H.; Kaler, L.; Herring, R. *J. Org. Chem.* **1984**, *49*, 2579.

(3) Electrophilic aromatic substitution reactions of PTAD frequently can be greatly facilitated by acid catalysis with trifluoroacetic acid: Wilson, R. M.; Hengge, A. C.; Ataei, A.; Chantarasiri, N. *J. Org. Chem.* **1990**, *55*, 193.

0002-7863/91/1513-2301$02.50/0